Technical Report

TR-2010-008

A data assimilation technique for including noisy measurements of the velocity field into Navier-Stokes simulations

by

M. D'Elia, A. Veneziani

Mathematics and Computer Science

EMORY UNIVERSITY

A DATA ASSIMILATION TECHNIQUE FOR INCLUDING NOISY MEASUREMENTS OF THE VELOCITY FIELD INTO NAVIER-STOKES SIMULATIONS

M. D'Elia*, A. Veneziani†

Dept. of Mathematics and Computer Science, Emory University,
400 Dowman Drive, Atlanta, GA 30322, USA
*e-mail: mdelia2@mathcs.emory.edu
†e-mail: ale@mathcs.emory.edu

Key words: Computational Fluid Dynamics, Optimization techniques, Inverse Problems, Data Assimilation, Hemodynamics

Abstract. *Including data into numerical simulations has always been an issue of paramount relevance in the prediction of fluid geophysics phenomena; due to advanced and efficient techniques in the field of biomedical imaging we can now collect a huge amount of measurements for the cardiovascular system. Our goal is to use these noisy and sparse data to get an accurate approximation of the blood flow in vessels in order to predict physical quantities of medical relevance. The combination of measurements and governing principles is known in literature as Data Assimilation (DA).*

In this work we propose a DA technique for including noisy measurements of the velocity field into the simulation of the Navier-Stokes (NS) equations driven by hemodynamics applications, since new devices make blood flow measurements available. Specifically, the technique we present is formulated as an inverse problem where, we use a Discretize then Optimize *(DO) approach to minimize the misfit between the recovered velocity field and the data, subject to the state equations; as a discretization technique the Finite Element (FE) method has been selected. The DA procedure for this nonlinear problem is a combination of two approaches: the Newton method for the NS equations, a common iterative procedure for the treatment of the nonlinear advection term, and the DA procedure we designed and tested for linear problems, specifically, for the Oseen problem. Our formulation is an iterative Newton-like procedure which exploits the DA technique for linear problems at each iteration.*

We present numerical results on a 2D NS test case, for which an exact flow is available; upon the introduction of a suitable noise, this is used for the generation of the data. We mainly focus on the error analysis: using noise-free data we check the consistency of our technique, recovering the FE convergence rates for the discretization error w.r.t. the exact solution. In the case of noisy data, we investigate the dependence of the discretization error on the amount of noise, the number and the location of measurements. We will show how the DA process improves the reliability of the numerical results on the primitive variable (velocity) and other flow-related variables of biomedical interest.

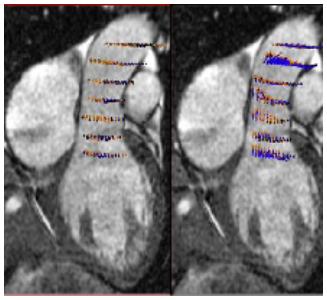

Figure 1: View of blood measured velocities in an MRI of the ascending aorta [11].

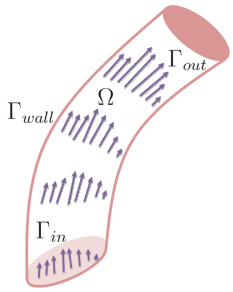

Figure 2: Possible 3D domain and data.

1 INTRODUCTION

Numerical methods for incompressible fluid dynamics have recently received strong impulse from applications to the cardiovascular system (see e.g. [5]). The integration of medical images and numerical simulations is fundamental for the development of clinically effective tools. The introduction and improvement of measurement and imaging devices enhances the integration process and opens new challenging goals; as an example Figure 1 reports an MRI [11] of the ascending aorta where blood velocity measurements have been collected. Beyond validation, these additional data can be used in numerical simulations to improve the accuracy of the recovered solution and increase the reliability of numerical results. While for hemodynamics this is a new field of investigation, the assimilation problem is well-known in other engineering fields; among those we mention geophysics and meteorology, where sparse and noisy data are combined with dynamic principles to get an accurate prediction of physical phenomena. The process of combining governing principles and data, which are sparse, irregularly distributed and subject to random noise is known in literature as Data Assimilation (DA).
In this paper we present a DA technique in computational fluid dynamics for including noisy measurements of the blood velocity into the simulation of the Navier-Stokes (NS) equations in a region of interest. For a brief overview of DA techniques during the last 50 years we refer to [10]. In Section 2 we present the mathematical formulation of the problem; in Section 3 we propose a DA procedure moving from the linear case to the nonlinear one; in Section 4 we present and discuss numerical results and in Section 5 we draw some conclusions and we present future research guidelines.

2 MATHEMATICAL FORMULATION OF THE DA PROBLEM

Given a domain $\Omega \in \mathbb{R}^2$, which represents the vessel of interest, we assume that on some internal and boundary points, $\mathbf{x}_i^m$, $i = 1, ..., N_d$, not necessarily in correspondence of grid nodes, a velocity measure is available (in Figure 2 a possible 3D domain is displayed); we call $\mathbf{d} \in \mathbb{R}^{2N_d}$ the vector of horizontal and vertical velocity measurements. Moreover, we denote by $\mathbf{u}(\mathbf{x})$ the velocity of the fluid, $p(\mathbf{x})$ the pressure field, Γ_{wall} the physical

boundary of the vessel, Γ_{in} and Γ_{out} the inflow and outflow sections. We assume that $\mathbf{u}(\mathbf{x}) \in \mathbf{H}^1(\Omega)$ and $p(\mathbf{x}) \in L^2(\Omega)$ satisfy the incompressible NS equations:

$$\begin{cases} -\nu\nabla\cdot(\nabla\mathbf{u}+\nabla\mathbf{u}^{\mathrm{T}})+(\mathbf{u}\cdot\nabla)\mathbf{u}+\nabla p=\mathbf{s} & \text{in } \Omega; \\ \nabla\cdot\mathbf{u}=0 & \text{in } \Omega, \end{cases} \tag{1}$$

with boundary conditions

$$\begin{cases} \mathbf{u}=\mathbf{0} & \text{on } \Gamma_{wall}; \\ -\nu(\nabla\mathbf{u}+\nabla\mathbf{u}^{\mathrm{T}})\cdot\mathbf{n}+p\cdot\mathbf{n}=\mathbf{h} & \text{on } \Gamma_{in}; \\ -\nu(\nabla\mathbf{u}+\nabla\mathbf{u}^{\mathrm{T}})\cdot\mathbf{n}+p\cdot\mathbf{n}=\mathbf{g} & \text{on } \Gamma_{out}. \end{cases} \tag{2}$$

Here, $\mathbf{h}(\mathbf{x}) : \mathbb{R}^2 \to \mathbb{R}^2$ and $\mathbf{g}(\mathbf{x}) : \mathbb{R}^2 \to \mathbb{R}^2$ are the Neumann data on the inflow and outflow boundaries; moreover, $\mathbf{h}$ is unknown.
Among available DA procedures, we formulate our assimilation technique as a control problem where we aim at minimizing the misfit between the predicted data and the data itself tuning the control variable $\mathbf{h}(\mathbf{x})$. In this framework, $\mathbf{u}$ and p are regarded as functions of $\mathbf{h}$. More precisely, let $dist(\mathbf{u}(\mathbf{h}), \mathbf{d})$ be the distance between the measured velocity data $\mathbf{d}$ and the recovered velocity $\mathbf{u}$ (to be specified later on). Given $\mathbf{d}$, our goal is to find $\mathbf{h}^*$ such that $dist(\mathbf{u}(\mathbf{h}^*), \mathbf{d}) \leq dist(\mathbf{u}(\mathbf{h}), \mathbf{d})$ for any feasible $\mathbf{h}$, under the constraint of (1) for $\mathbf{u}(\mathbf{h})$ and $p(\mathbf{h})$.

3 NUMERICAL SOLUTION OF THE DA PROBLEM

For the numerical solution of the optimization problem we first focus on the linear Oseen problem (i.e. we replace the nonlinear term $(\mathbf{u}\cdot\nabla)\mathbf{u}$ in (1) with $(\boldsymbol{\beta}\cdot\nabla)\mathbf{u}$, being $\boldsymbol{\beta}$ a given convective field).
Here, we follow a Discretize-then-Optimize (DO) procedure. Other approaches are possible, however preliminary results suggest that DO is the most effective (see [2]). In the DO procedure we first discretize the minimization problem subject to the Oseen equations using the Finite Element (FE) method with a suitable choice of compatible FE space [9]; then, we solve the induced algebraic optimization problem. Let us introduce the following notations,

$$\mathbf{V}=\begin{bmatrix}\mathbf{U}\\ \mathbf{P}\end{bmatrix},\quad \mathrm{D}=[\mathrm{Q}\ \ \mathrm{O}];\quad \mathrm{S}=\begin{bmatrix}\mathrm{C} & \mathrm{B}^{\mathrm{T}}\\ \mathrm{B} & \mathrm{O}\end{bmatrix},\quad \mathrm{R}=\begin{bmatrix}\mathrm{N}\\ \mathrm{O}\end{bmatrix}, \tag{3}$$

where $\mathbf{U} \in \mathbb{R}^{N_u}$, $\mathbf{P} \in \mathbb{R}^{N_p}$ and $\mathbf{H} \in \mathbb{R}^{N_h}$ are the discretized velocity, pressure and flux vector; let C and B be the discretization of the advection-diffusion and divergence operators and N the discretization of the mass operator computed only on inlet boundary nodes. More specifically, the matrix N comes from the discretization of the term $\int_{\Gamma_{in}} \mathbf{h}\,\mathbf{v}\,\mathrm{d}\sigma$ coming from integration by parts in the weak formulation of the problem. Also, Q is a selection matrix designed such that $[\mathrm{Q}\mathbf{U}]_i$ is the numerical solution corresponding to $\mathbf{d}_i$

(i.e. in the same location). Specifically, when measurement nodes do not correspond to grid points, $[\mathrm{Q}\mathbf{U}]_i$ is the value of the FE numerical solution evaluated at $\mathbf{x}_i$ obtained by a weighted sum of the FE basis functions. Upon discretization, the algebraic minimization problem reads,

$$\begin{aligned} &\min \frac{1}{2}\|\mathrm{D}\mathbf{V}-\mathbf{d}\|_2^2+\frac{a}{2}\|\mathrm{L}\mathbf{H}\|_2^2 \\ &\text{s.t. } \mathrm{S}\mathbf{V}=\mathrm{R}\mathbf{H}+\mathbf{F}. \end{aligned} \tag{4}$$

Here a regularization term has been added to the functional due to the possible ill-posedness or ill-conditioning of the problem, possibly caused by the position of the data and pinpointed by the amount of noise; L is the discretization of a regularization operator (e.g. the gradient).
For the solution of problem (4), we write the Lagrangian and we solve the associated set of equations, coming from the optimality necessary conditions. The Lagrangian reads

$$\mathcal{L}(\mathbf{V},\mathbf{H},\mathbf{\Lambda})=\frac{1}{2}\|\mathrm{D}\mathbf{V}-\mathbf{d}\|_2^2+\frac{a}{2}\,\|\mathrm{L}\mathbf{H}\|_2^2+\mathbf{\Lambda}^{\mathrm{T}}(\mathrm{S}\mathbf{V}-\mathrm{R}\mathbf{H}-\mathbf{F}); \tag{5}$$

where $\mathbf{\Lambda}\in\mathbb{R}^{N_u+N_p}$ is the Lagrangian multiplier. The set of necessary conditions for the optimality is given by

$$\begin{cases} \mathrm{D}^{\mathrm{T}}(\mathrm{D}\mathbf{V}-\mathbf{d})+\mathrm{S}^{\mathrm{T}}\mathbf{\Lambda}=0; \\ a\mathrm{L}^{\mathrm{T}}\mathrm{L}\mathbf{H}-\mathrm{R}^{\mathrm{T}}\mathbf{\Lambda}=0; \\ \mathrm{S}\mathbf{V}-\mathrm{R}\mathbf{H}=\mathbf{F}. \end{cases} \tag{6}$$

Upon block elimination, the reduced system reads

$$(\mathrm{R}^{\mathrm{T}}\mathrm{S}^{-\mathrm{T}}\mathrm{D}^{\mathrm{T}}\mathrm{D}\mathrm{S}^{-1}\mathrm{R}+a\mathrm{L}^{\mathrm{T}}\mathrm{L})\mathbf{H}=\mathrm{R}^{\mathrm{T}}\mathrm{S}^{-\mathrm{T}}\mathrm{D}^{\mathrm{T}}\mathbf{d}. \tag{7}$$

By defining $\mathrm{Z}=\mathrm{D}\mathrm{S}^{-1}\mathrm{R}$ system (7) reads

$$(\mathrm{Z}^{\mathrm{T}}\mathrm{Z}+a\mathrm{L}^{\mathrm{T}}\mathrm{L})\mathbf{H}=\mathrm{Z}^{\mathrm{T}}\mathbf{d}, \tag{8}$$

where Z, can be regarded as $\mathrm{Z}=\partial\mathrm{D}\mathbf{V}(\mathbf{H})/\partial\mathbf{H}$, the so-called *sensitivity* matrix. The spectral properties of this matrix determine the conditioning of the problem.

3.1 DA procedure for the NS problem

For the solution of the DA problem for the NS equations we combine the DA procedure for linear problems presented in Section 3 and a fixed point method for the solution of the NS equations; in particular, we employ both Picard and Newton methods (for the formulation of the two techniques we refer to [8]).
We solve the DA problem iteratively: given an initial guess for the discrete velocity $\mathbf{U}$, at

each step we minimize the functional in (4) subject to the constraint given by a Picard or Newton iteration. More precisely, in the following we set

$$\mathrm{S}_k = \begin{bmatrix} \mathrm{C} + \mathrm{A}_k & \mathrm{B}^{\mathrm{T}} \\ \mathrm{B} & \mathrm{O} \end{bmatrix}, \qquad \mathbf{F}_k = \mathbf{F} + w\mathbf{Y}_k, \tag{9}$$

where A_k and Y_k are related to the linearization of the NS equations. Specifically, A_k is the FE matrix coming from the discretization of the term $(\mathbf{u}_k \cdot \nabla)\mathbf{u}_{k+1} + w(\mathbf{u}_{k+1} \cdot \nabla)\mathbf{u}_k$ and $\mathbf{Y}_k$ is the vector coming from the discretization of $(\mathbf{u}_k \cdot \nabla)\mathbf{u}_k$. The coefficient $w \in [0,\, 1]$ activates the Newton process: $w = 0$ corresponds to classical Picard iterations, $w \in (0,\, 1)$ to relaxed Newton iterations and $w = 1$ to pure Newton iterations. The algorithm reads:

Algoritm 1. Given an initial guess $\mathbf{U}_0$

do

$$\begin{aligned} &solve : \min \frac{1}{2}\|\mathrm{D}\mathbf{V}_{k+1} - \mathbf{d}\|_2^2 + \frac{a}{2}\|\mathrm{L}\mathbf{H}_{k+1}\|_2^2 \\ &\qquad \text{s.t. } \mathrm{S}_k\mathbf{V}_{k+1} = \mathrm{R}\mathbf{H}_{k+1} + \mathbf{F}_k; \\ &k = k + 1; \end{aligned}$$

while $(\|\mathbf{U}_k - \mathbf{U}_{k+1}\| \geq \delta)$.

The parameter δ is a user-defined tolerance.
Since the Newton method is only locally convergent, a good initial guess $\mathbf{U}_0$ is required; a common procedure is to perform a few Picard iterations and use the resulting velocity as an initial guess (we refer to this method as Picard-Newton).

4 NUMERICAL RESULTS

In this Section we present numerical results obtained performing the DA procedure on the NS problem. Using noise free data we verify the consistency of Algorithm 1 with both Picard and Picard-Newton iterations. Then, we introduce noisy data for investigating the dependence of the discretization error on the number of data, their location and the amount of noise. Also, we present numerical results in a curved domain pointing out the accuracy of the vector assimilated with the noisy data. The computation of an index of hemodynamic interest such as the Wall Shear Stress (WSS) is also reported.

4.1 An analytical test case

All simulations presented in this Section are based on the 2D NS flow in the domain $\Omega = [-0.5,\, 1.5] \times [0,\, 2]$ whose analytical solution reads

$$\begin{cases} [\mathbf{u}]_1(x,y) = 1 - e^{\lambda x}\cos(2\pi y), \\ [\mathbf{u}]_2(x,y) = \dfrac{\lambda}{2\pi} e^{\lambda x}\sin(2\pi y), \\ p(x,y) = \dfrac{1}{2}e^{2\lambda x} + C. \end{cases} \tag{10}$$

Here, the viscosity of the fluid is $\nu = 0.035\, m^2/s$, the adimensional parameter λ is such that $\lambda = \frac{1}{2}(\nu^{-1} - \sqrt{\nu^{-2} + 16\pi^2})$, and C is a constant chosen to give a zero mean pressure.

Data Generation We assume data to be given on the inflow boundary and on some internal points in the computational domain, not necessarily in correspondence of grid points. These data are generated adding white noise uniformly distributed in space (globally) to the exact solution. In this procedure we fix the Signal-to-Noise Ratio, SNR; this fact determines the parameters of the noise probability distribution in the generation process. In real applications this value is strongly determined by the biomedical tools used to observe the data. In the case of noisy data from a 4D scan of the aorta, SNR can be as low as 10 for flow measures (personal communication of Dr. M. Brummer).

Implementation details We implement the FE method with choice of compatible FE spaces P1bubble-P1 for velocity and pressure respectively. For our DO approach we use the regularizing operator $\mathrm{L} = \nabla_d$ (a discretization of the gradient) and we generate the optimal parameter by means of the Discrepancy Principle (DP) [7]. With noise free data, the optimal regularization parameter is of the order of 10^{-9} and no regularization is used; note that the location of measurement nodes affects the well-posedness and the conditioning of the problem in a nontrivial way (see Section 4.2 and [3] for more details). A critical step in the DA procedure is the solution of system (8). We rely on the GMRES method; its bottleneck is the solution of linear systems associated with S and S^{T} where an efficient preconditioner is required; we solve these systems monolithically with the Pressure-Advection-Diffusion preconditioner introduced by Elman et al. in [4]. Table 1 reports stopping criteria used for each linear system involved. $Prec(\mathrm{S}_k)$ stands for the preconditioned system; also, $\mathbf{r}(\mathbf{x})$ is the residual at the current iteration and **rhs** is the right hand side of the current system.
Numerical results are obtained with the C++ FE library lifeV [1] and post-processed with ParaView [2].

[1] Free C++ library, which the authors are developers of, available on www.lifev.org.

[2] An open-source, multi-platform application designed to visualize data sets, available on www.paraview.org.

system	solver	toll	stopping criteria
S_k	GMRES	1.e-9	$\|\mathbf{r}(\mathbf{x})\|/\|\mathbf{r}(\mathbf{x}_0)\|$
$Prec(S_k)$	GMRES	1.e-9	$\|\mathbf{r}(\mathbf{x})\|/\|\mathbf{rhs}\|$
Z^TZ	GMRES	1.e-6	$\|\mathbf{r}(\mathbf{x})\|/\|\mathbf{rhs}\|$

Table 1: Parameters setting for the iterative solvers (implemented in the external library AZTEC).

method	$h = 0.16$			$h = 0.072$			$h = 0.05$		
	$E_{\mathbf{U}}$	t	it	$E\mathbf{U}$	t	it	$E\mathbf{U}$	t	it
Picard	4.98e-2	23	6	9.59e-3	540	5	4.79e-3	4680	5
Picard-Newton	4.97e-2	20	5 (3)	9.49e-3	780	4 (2)	4.73e-3	5600	4 (2)

Table 2: Numerical results using Picard iterations and Picard-Newton iterations. In brackets, the number of Picard iterations to get the initial guess.

4.2 Error analysis with noise free data

In order to investigate consistency of our method, using noise free data we analyze the discretize-error with respect to the exact solution. In this case we have to recover the FE error convergence rate as a function of the discretization parameter Δx. In this test case the set of measurement points is a subset of the set of grid nodes; specifically, we consider data on Γ_{in} and on three internal layers (in correspondence of $x = 0,\ 0.5,\ 1$).
In Table 2 we report for Picard and Picard-Newton iterations the discretization error

$$E_{\mathbf{U}} = \frac{\|\mathbf{U} - \mathbf{U}_{ex}\|_2}{\|\mathbf{U}_{ex}\|_2} \tag{11}$$

and the number of iterations of Algorithm 1 (in the case of Picard-Newton it corresponds to the sum of Picard iterations performed to obtain the initial guess and Newton iterations to get convergence, the latter is reported in brackets). Same results are reported in Figure 3 in a loglog scale with a reference quadratic curve. With both techniques we recover the expected FE convergence rate; also, for each mesh the Newton method yields a slightly better accuracy. Moreover, we observe that the number of iterations needed for the convergence is almost mesh independent and that, as expected, the Newton method requires less iterations to satisfy the stopping criteria. A deeper theoretical investigation is needed to prove that it preserves its quadratic convergence when combined with the DA procedure. In Figure 4 (left) we report the computed pressure and velocity field obtained in correspondence of $\Delta x = 0.072$ after four Picard-Newton iterations. The recovered velocity field matches accurately the data, represented by the white vector field on Γ_{in} and on three internal layers.

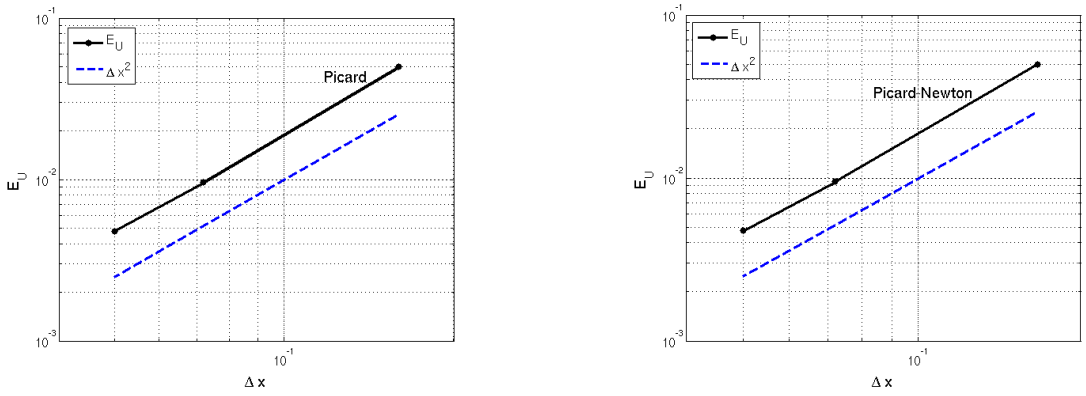

Figure 3: Relative errors $E_{\mathbf{U}}$ versus Δx for Picard (left) and Picard-Newton (right) iterations with noise free data.

4.3 Error analysis with noisy data

In this Section we consider the case of noisy data and we investigate the dependence of the discretization error on the number of available measures, on their position and on the amount of noise.

In Table 3 we report the discretization error and the number of iterations performed by Algorithm 1 in correspondence of SNR = 20 for different numbers of measurement points N_d; no regularization is used in this case. For this simulation we still sample the data on Γ_{in} and on three internal layers. In Figure 4 (right) we report the computed field and the noisy data: the presence of the noise is evident in the vertical components. In particular, we notice that the noise mainly affects low magnitude velocities; this happens since the amount of noise does not depend on the local magnitude of the velocity vector field. In correspondence of these low magnitude values the recovered assimilated field differs significantly from the data and it is closer to the exact solution thanks to the assimilation process.

In Figure 5 (left) we report the error and a reference curve $\mathcal{O}(\sqrt{N_d^{-1}})$. We note that, for a given set of n independent identically distributed random variables, the standard deviation is proportional to $\sqrt{n^{-1}}$; this explains our results.

In Figure 5 (right) we report in a loglog scale the discretization error versus the inverse of the signal to noise ratio for SNR = $\{33.3, 20, 10, 8.3\}$. We can notice a linear behavior by a comparison with the dashed reference curve. As SNR gets smaller, more Newton iterations are required to reach convergence; we can infer that a higher amount of noise affects the conditioning of the problem.

The number of available measures on the inflow boundary and the additional availability of internal measurements affects the quality of the solution in terms of accuracy and well-conditioning of the numerical problem [3]. This is verified in the following tests performed on the domain Ω defined above, related results are reported in Table 4.

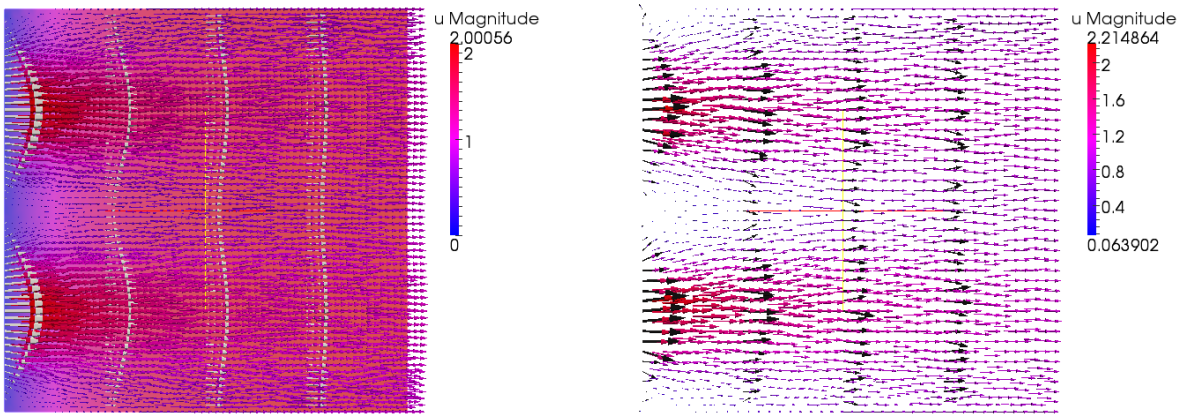

Figure 4: On the left, the computed pressure and velocity vector field with the noise-free data (white vector field). On the right the computed pressure and velocity vector field with the noisy data (black vector field) for SNR = 20.

- test 1. data on all grid nodes on Γ_{in};
- test 2. data on half of the grid nodes on Γ_{in};
- test 3. data on 12 points (not necessary grid nodes) on on Γ_{in};
- test 4. data on all grid nodes on Γ_{in} and 30 points $\mathbf{x} \in [-0.5,\, 0] \times [0,\, 2]$;
- test 5. data on all grid nodes on Γ_{in} and 30 points $\mathbf{x} \in [1,\, 1.5] \times [0,\, 2]$;
- test 6. data on all grid nodes on Γ_{in} and 30 points $\mathbf{x} \in [-0.5,\, 1.5] \times [0,\, 2]$;

Here, we use $\Delta x = 0.072$ and SNR $= 20$. Regularization is required by the ill-conditioning of the problem which gets worse as we decrease the number of available measurements on Γ_{in}; further investigation on the relation between the well-posedness (or conditioning) of the problem and the displacement of the data will be addressed in [3]. From these results we notice that the number of iterations required to reach convergence is not related to the number of available measurements and neither to the conditioning of the problem; however, it affects the number of GMRES iterations in the solution of the single optimization problem and the accuracy of the computed solution. Accuracy is improved by regularization; this happens because of the smoothing and filtering properties of the regularizing term. Finally, we notice that the availability of additional measurements at some internal points (not necessarily in correspondence of grid nodes) improves the accuracy of the solution. Also, in this specific case, a uniform distribution of internal measurement nodes yields a slightly better accuracy.

SNR	$N_d = 48$			$N_d = 112$			$N_d = 160$		
	E	t	it	E	t	it	E	t	it
20	6.95e-2	28	5 (3)	3.96e-2	3240	5 (2)	2.97e-2	4740	4 (2)

Table 3: Numerical results using Newton-Picard iterations.

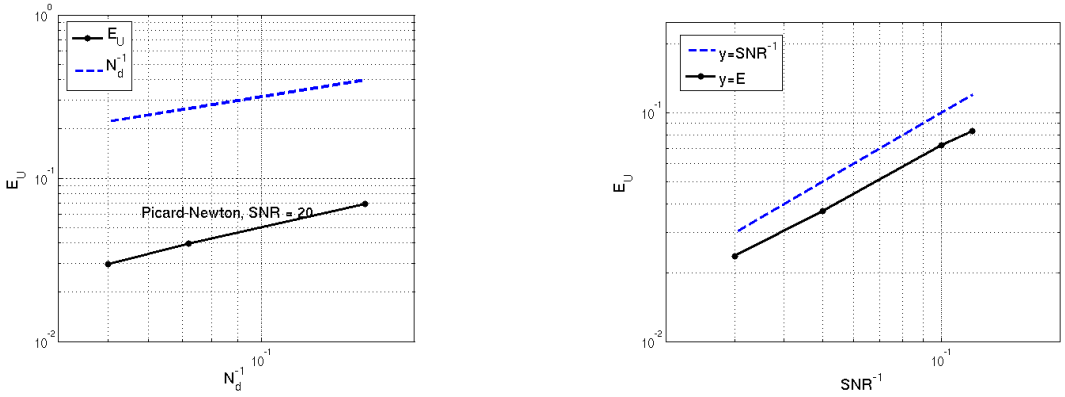

Figure 5: Relative errors $E_{\mathbf{U}}$ versus Δx with noisy data (left); relative errors $E_{\mathbf{U}}$ versus SNR^{-1} (right) for Picard-Newton iterations.

4.4 Towards real geometries

In this Section we want to focus on a more complex geometry; in particular, we want to reproduce in a 2D computational domain a section of the aortic arc, which is the vessel we are mainly interested in and where we assume to have some velocity measurements as in Figure 1. Specifically, we introduce the computational domain, we describe a new data generation procedure and we report some results obtained with the DA technique for the NS formulation. As done previously, we use compatible FE spaces P1bubble-P1 for the approximation of the velocity and pressure fields and we rely on the software FreeFem++ for the mesh generation. In Figure 6 (left) we report the computational domain, which is a rough approximation of a section of the ascending aorta. We assume to have velocity measurements on the inflow boundary Γ_{in} and on three internal layers Γ_{data}, as shown in Figures 6 and 7 (left) for noise free and noisy data. Also, we prescribe homogeneous Dirichlet boundary conditions on Γ_{wall} and homogeneous Neumann boundary conditions on the outflow boundary Γ_{out}. As anticipated above, a new data generation procedure needs to be designed, since the analytic solution is not available. As a reference solution we use a numerical solution, computed with the FE method on a very fine grid, which can be considered a reliable approximation of the exact solution. For the computation of this approximate solution, which we call $\mathbf{U}_{\text{FE}}$, we prescribe the following boundary conditions,

test	$E_{\mathbf{U}}$	it
1	5.074e-2	4
2	7.334e-2	4
3	7.664e-2	4

test	$E_{\mathbf{U}}$	it
1	4.748e-2	4
2	6.590e-2	4
3	6.679e-2	4
4	3.860e-2	4
5	4.414e-2	4
6	3.161e-2	4

Table 4: Numerical results for noisy data with SNR = 20 without (left) and with (right) regularization.

being $k = 1$,

$$\mathbf{u} = \mathbf{0} \text{ on } \Gamma_{wall}; \qquad -\nu\frac{\partial \mathbf{u}}{\partial \mathbf{n}} + p = 0 \text{ on } \Gamma_{out}; \qquad \mathbf{u} = [\,0 \;\; k(r_2 - x)(x - r_1)\,]^T \text{ on } \Gamma_{in}. \quad (12)$$

$\mathbf{U}_{\mathrm{FE}}$ is used both for data generation and error evaluation. More specifically, the data are generated adding a random noise to $\mathrm{P}\mathbf{U}_{\mathrm{FE}}$; here, P is a projector of the FE solution computed on a finer grid on the FE space associated with the current computational grid. In this way, the reference solution is affected both by the FE approximation error and the projection one. This fact, anyway, does not affect the reliability of our results; in fact, the FE approximation error and the projection one can be regarded as part of the noise of our data. We measure the error by computing the following index

$$\frac{\|\mathbf{U} - \mathrm{P}\mathbf{U}_{\mathrm{FE}}\|_{L^2}}{\|\mathbf{U}_{\mathrm{FE}}\|_{L^2}}.$$

In Figure 6 (right) we report the pressure and velocity vector field, computed with the DA technique, together with the noise-free data: the velocity matches the data in correspondence of the internal layers. In Figure 7 (right) we report the computed pressure and velocity vector field with a noisy data generated with SNR = 10; which is a realistic value for true instrumental noise. In this case, the noise mainly affects the components of the velocity which are transversal to the flow (they are supposed to be close to zero). Despite this, the recovered field is close to the reference solution; this confirms the noise-filtering property of the DA process.

The wall shear stress Finally, we want to consider the computation of the Wall Shear Stress (WSS) which is a quantity of medical interest . It is defined as the tangent component of the stress exerted by the fluid (blood in this case) on the arterial wall; formally

$$\boldsymbol{\tau} = \nu(\nabla\mathbf{u} + \nabla\mathbf{u}^{\mathrm{T}})\mathbf{n} - \nu\left(\left((\nabla\mathbf{u} + \nabla\mathbf{u}^{\mathrm{T}})\mathbf{n}\right)\cdot\mathbf{n}\right)\mathbf{n}, \quad (13)$$

where $\mathbf{n}$ is the normal vector in correspondence of the wall. An accurate approximation of the WSS is fundamental in the investigation of cardiovascular pathologies since it is an

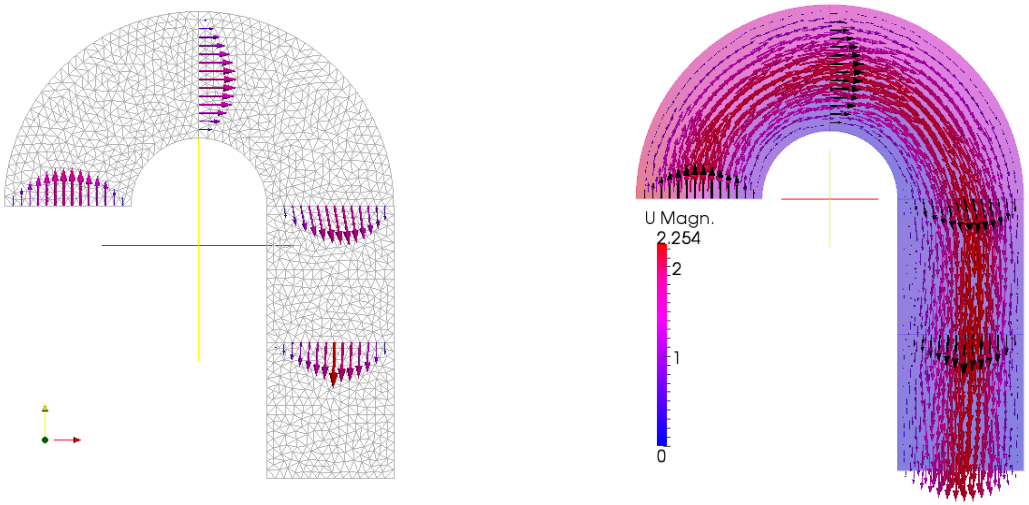

Figure 6: On the left, computational mesh reproducing the aortic arc and noise free data. On the right, pressure and velocity fields recovered from noise free data.

index of the possibility of rupture of the vessel wall and of the formation of stenosis [5]. Approximations of the WSS retrieved from indirect measurements velocities are in general unreliable because of post-process operations and the noise affecting the measures. DA can be considered a way for improving the reliability of this computation thanks to the noise-filtering due to the introduction of the numerical blood flow model. In Figure 8 we report a comparison between the WSS computed using the reference solution $\mathrm{P}\mathbf{U}_{\mathrm{FE}}$ and the one computed upon assimilated velocities; we note that by means of DA the recovered WSS catches accurately the behavior of the reference one. These preliminary results pinpoint the role of DA as a way for filtering and eventually computing hemodynamical indexes with good accuracy.

5 CONCLUSIONS

On the basis of a DA procedure for linear problems we developed an efficient algorithm for the integration of noisy data and the numerical simulation of the NS equations. The combination of Picard and Newton iterations in Algorithm 1 yields convergence after few iterations. However, the computational effort is still high and the numerical solution can be improved employing a more efficient preconditioner for the Oseen problem. A possible choice is the Augmented Lagrangian preconditioner which can either improve the conditioning and stabilize possible advection dominated phenomena [1].
As expected, the noise affects both the accuracy of the solution and the efficiency of the procedure. Also, data location plays a fundamental role in the well-conditioning of the formulation: numerical tests proved that both regularization and a suitable measurements distribution might improve the spectral properties of the problem (more details will be reported in [3]).

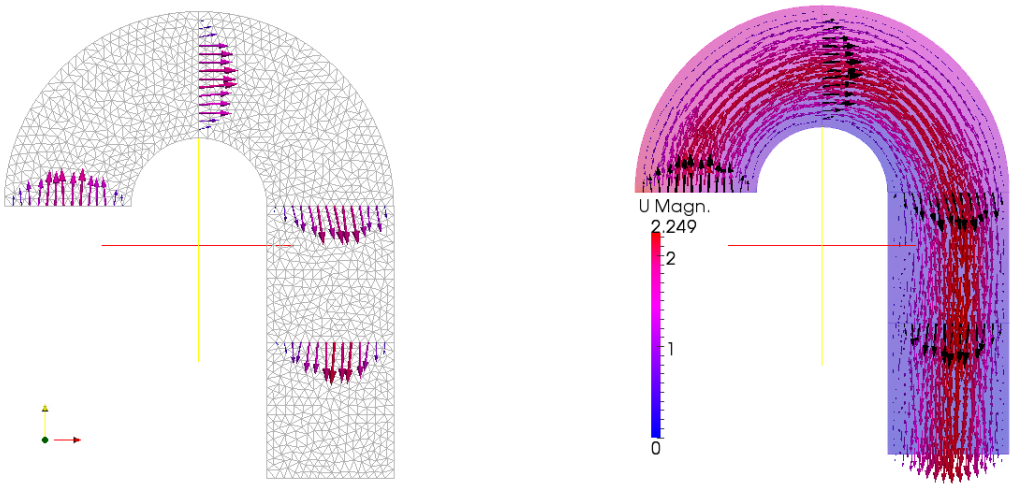

Figure 7: On the left, computational mesh reproducing the aortic arc and noise free data. On the right, pressure and velocity fields recovered from noise free data.

The well-posedness of the formulation and an estimate of the discretization error related to the noise level are the subject of future theoretical investigation. Under a computational perspective, we aim at improving the efficiency of the numerical procedure in the solution of the control problem and to test our method on real data and 3D geometries.

REFERENCES

[1] M. Benzi, M. Olshanskii, Z. Wang, Modified Augmented Lagrangian Preconditioners for the Incompressible Navier-Stokes Equations. *International Journal for Numerical Methods in Fluids* (2010); DOI: 10.1002/fld.2267.

[2] M. D'Elia, A. Veneziani, Methods for assimilating blood velocity measures in hemodynamics: preliminary results, accepted for publication on *Procedia Computer Science*, (2010).

[3] M. D'Elia, M. Perego, A. Veneziani, in preparation, (2010).

[4] H. Elman, D. Silvester , A. Wathen, Finite Elements and Fast Iterative Solvers with applications in incompressible fluid dynamics, *Numerical Mathematics and Scientific Computation*, Oxford University Press, New York, (2005).

[5] L. Formaggia, A. Quarteroni, A. Veneziani, Cardiovascular Mathematics, *Modeling and simulation of the circulatory system*, MS&A **1**, (2009).

[6] M.D. Gunzburger, Perspectives in Flow Control and Optimization, *Society for Industrial Mathematics*, (2002).

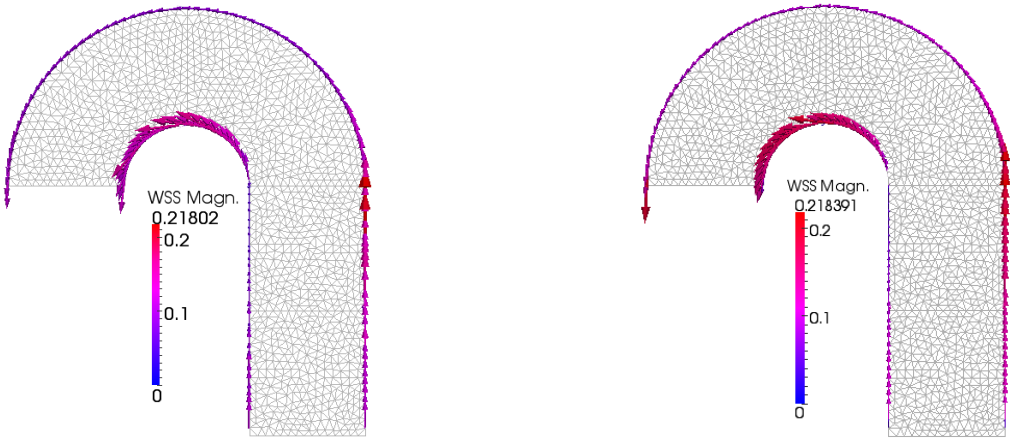

Figure 8: Comparison between the map of the stress exerted by the blood in the arterial wall recovered from the reference solution, on the left, and from noisy velocity data of Figure 7 (left), on the right.

[7] P.C. Hansen, Rank-deficient and discrete ill-posed problems: numerical aspects of linear inversion, *Society for Industrial and Applied Mathematics*, (1998).

[8] A. Quarteroni, R. Sacco, F. Saleri, Numerical Mathematics, *Texts in Applied Mathematics*, Springer, (2000).

[9] A. Quarteroni, A. Valli, Numerical Approximation of Partial Differential Equations, *Springer Series in Computational Mathematics*, Springer,(1997).

[10] A.R. Robinson, P.F.J. Lermusiaux. Overview of data assimilation. *Technical Report* **62**, Harvard University, Cambridge, (2000).

[11] P. van der Velden, D. Sallee, E. Zaaijer, W.J. Parks, S. Ramamurthy, T.Q. Robbie, J. Huckaby, S. Chochua, M.E. Brummer, Systolic flow jet is an indicator of aortic root dilation for bicuspid aortic valves, *Poster* (2008).